Negative Ion Photoelectron Spectroscopy of $NH_2^-(NH_3)_1$ and $NH_2^-(NH_3)_2$: Gas Phase Basicities of Partially Solvated Anions

Joseph T. Snodgrass,[†] James V. Coe,[‡] Carl B. Freidhoff,[§] Kevin M. McHugh,[||] Susan T. Arnold,[⊥] and Kit H. Bowen*

Department of Chemistry, Johns Hopkins University, Baltimore, Maryland 21218

Received: November 15, 1994; In Final Form: February 7, 1995[⊗]

The photoelectron spectra of the gas phase negative cluster ions $NH_2^-(NH_3)_1$ and $NH_2^-(NH_3)_2$ are reported. The spectra imply that these ions consist of intact amide ions solvated by ammonia. Vertical detachment energies and ion–solvent dissociation energies are obtained. In addition, spectral features are also observed that indicate that the ammonia moiety in these cluster anions is distorted from the equilibrium configuration of the free ammonia molecule. The spectra are compared to the photoelectron spectra of $H^-(NH_3)_1$ and $H^-(NH_3)_2$. Gas phase basicities are determined for $NH_2^-(NH_3)_1$, $NH_2^-(NH_3)_2$, $H^-(NH_3)_1$, and $H^-(NH_3)_2$. While NH_2^- is a stronger base than H^- in the gas phase, our data show that the addition of only two ammonia solvent molecules reverses the relative basicities of these two species.

Introduction

The governing influence of solvation on the energetics, equilibria, and rates of chemical reactions occurring in solution has long been recognized.[1–3] There are many cases in which a change in solvent medium changes the rate or equilibrium constant of a reaction by several orders of magnitude.[4] In order to understand solution phase chemistry, a knowledge of the primary reaction chemistry must be supplemented by information on the interactions between reactant and product molecules with the solvent. Distinguishing between the intrinsic properties of reacting chemical species and the effects attributable to solvation, however, is often difficult.

The development in the mid-1960s of experimental methods for studying ion–molecule reactions in the gas phase, in the absence of a solvent medium, profoundly influenced our understanding of chemical reactivity.[5–9] Using ion cyclotron resonance mass spectrometry,[7] high-pressure mass spectrometry,[8] and flowing afterglow methods,[9] it became possible to make thermodynamic and kinetic measurements for a wide variety of chemical reactions without the complicating effects of solvation. Since solvation energies are often large enough to dominate over differences in intrinsic reactivities, the data generated revealed subtle yet important chemical differences for the first time. During the course of these studies, gas phase acid–base chemistry received considerable attention.[5,6,10–16] By measuring equilibrium constants for proton transfer reactions, relative acidities and basicities were determined and anchored to an absolute scale (see tables in refs 5, 6, and 16). Of particular significance, it was found that the ordering of relative acidities for a number of alcohols in the gas phase is the reverse of their ordering in solution.[14] Likewise, for a given list of related bases, it was found that the ordering of their basicities in the gas phase often differs from their ordering in solution.[15]

In addition to information on intrinsic reactivities, information on the interactions between ions and solvent molecules has also been obtained.[17–22] By measuring equilibrium constants as a function of temperature for solvation reactions, i.e.,

$$A^{\pm}(S)_n + S + M \rightarrow A^{\pm}(S)_{n+1} + M$$

sequential ion–solvent dissociation enthalpies and entropies have been determined via van't Hoff plots. The utility of such data in understanding ion solvation has been reviewed,[19–21] and a comprehensive compilation is available.[22] The vast majority of such measurements have been made using high-pressure mass spectrometry and flowing afterglow methods. More recently, the determination of ion–solvent bond dissociation energies from the photoelectron spectra of negative cluster anions has also been demonstrated.[23,24] An additional benefit of using a spectroscopic approach is the possibility of obtaining structural information as well as qualitative information on the nature of bonding between anions and neutral solvents.

In this paper, we report the results of our investigation on the cluster anions $NH_2^-(NH_3)_1$ and $NH_2^-(NH_3)_2$ by negative ion photoelectron spectroscopy. The $NH_2^-(NH_3)_1$ ion is an ion–molecule complex of a strong base, NH_2^-, with its conjugate acid, NH_3. Solvation decreases the effective basicity of a gas phase ion. In this study, we measure the extent of this decrease with sequential solvation. This work is complimentary to our previously reported study of $H^-(NH_3)_{n=1,2}$ cluster anions,[23] which we review in the context of acid–base chemistry, the emphasis of this study.

Experimental Section

In continuous beam negative ion photoelectron spectroscopy, a steadily operating mass-selected beam of negative ions is crossed with a fixed-frequency photon beam, and the resultant photodetached electrons are energy-analyzed. Subtraction of the center-of-mass electron kinetic energy of an observed spectral feature from the photon energy gives the transition energy (the electron binding energy) from an occupied level in the negative ion to an energetically accessible level in the corresponding neutral. Our apparatus, which has been described previously,[25] employs a Wien velocity filter for mass selection, an argon ion laser operated intracavity in the ion–photon

[†] Present address: American Cyanamid Company, Princeton, NJ 08543-0400.
[‡] Present address: Department of Chemistry, Ohio State University, Columbus, OH 43210.
[§] Present address: Westinghouse Research and Development Center, Pittsburgh, PA 15235.
[||] Present address: National Engineering Laboratory, Idaho Falls, ID 83401.
[⊥] Present address: Phillips Laboratory (GPID), Hanscom Air Force Base, MA 01731.
* Corresponding author.
[⊗] Abstract published in *Advance ACS Abstracts,* April 1, 1995.

0022-3654/95/2099-9675$09.00/0

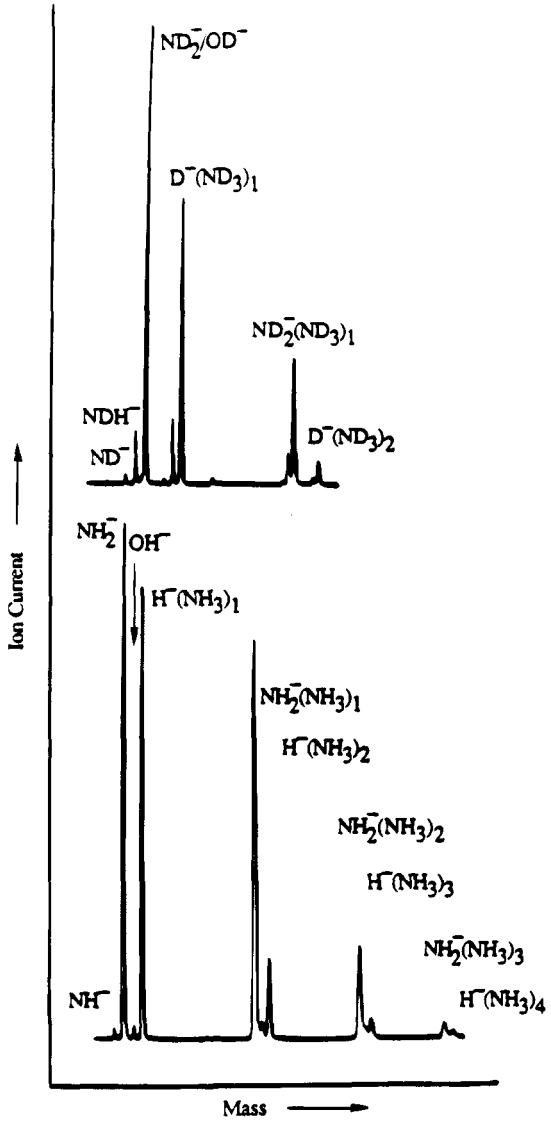

Figure 1. Typical mass spectrum obtained by using ND_3 and NH_3 in our supersonic expansion ion source.

interaction region, and a magnetically shielded, hemispherical electron energy analyzer.

Negative cluster ions of $NH_2^-(NH_3)_n$ were generated using a supersonic expansion ion source. The operation of this source involves the injection of electrons from a biased hot filament into an expanding supersonic jet in the presence of magnetic fields. Typical source operation conditions were as follows: a nozzle diameter of 18 μm, a stagnation pressure of 30 psig of ammonia, a beam voltage of -500 V, a filament bias of -70 V relative to the nozzle, a filament emission of ca. 15 mA, an extraction voltage of ca. 1300 V, and a nozzle temperature of ca. 0 °C. Currents measured at the Faraday cup beyond the ion–photon interaction region were usually ca. 2×10^{-9} A of $NH_2^-(NH_3)_1$ and ca. 5×10^{-10} A of $NH_2^-(NH_3)_2$. Typical mass spectra obtained by using neat NH_3 and ND_3 are presented in Figure 1 on aligned mass scales. Mass assignments were confirmed by photodetaching ions with well-known photoelectron spectra such as NH_2^- and OH^-. As shown in Figure 1, cluster ions of the $H^-(NH_3)_n$ cluster ion series were also produced under these conditions.

Results and Interpretation of Spectra

1. Data. The photoelectron spectra of NH_2^-, $NH_2^-(NH_3)_1$, and $NH_2^-(NH_3)_2$ are presented in Figure 2, all on aligned center-

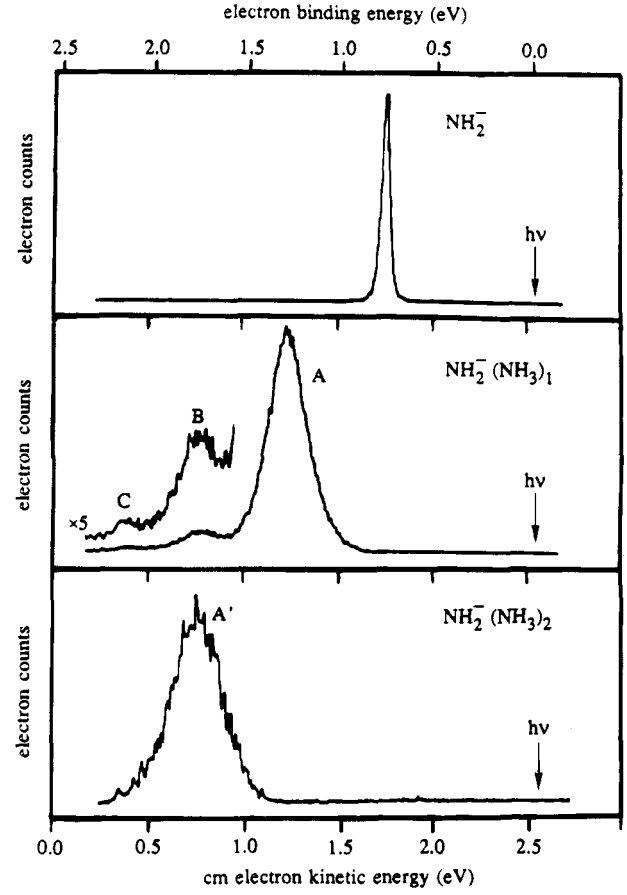

Figure 2. Photoelectron spectra of NH_2^-, $NH_2^-(NH_3)_1$, and $NH_2^-(NH_3)_2$, each recorded with 2.540 eV photons.

of-mass (cm) electron kinetic energy scales. The inset above the $NH_2^-(NH_3)_1$ spectrum is a magnified trace of the low electron kinetic energy portion of the spectrum. The photoelectron spectrum of $ND_2^-(ND_3)_1$ was also recorded. In all the spectra shown here, the photon energy was 2.540 eV, the electron energy channel spacing was 8.5 meV, and the electron energy analyzer's instrumental resolution was 30 meV. The mass resolution typically used in these experiments was that shown in Figure 1. The photoelectron spectrum of OH^- was recorded before and after each $NH_2^-(NH_3)_n$ spectrum to calibrate the electron energy analyzer's energy scale. The ND_2^- ion's photoelectron spectrum served as the calibrant for the $ND_2^-(ND_3)_1$ spectrum. The NH^- photoelectron spectrum was also recorded periodically to determine the electron energy analyzer's compression factor, which was always found to be between 1.000 and 1.020. Table 1 summarizes peak positions, intensities, and widths as determined by fitting the experimental data to asymmetric Gaussian peak shapes.

The photoelectron spectra of $NH_2^-(NH_3)_1$ and $NH_2^-(NH_3)_2$ are both dominated by large peaks, which are designated as peaks A and A′, respectively, in Figure 2. The $NH_2^-(NH_3)_1$ spectrum also exhibits two smaller peaks on the low electron kinetic energy side (the high electron binding energy side) of peak A, and these are designated as peaks B and C. Also, the $NH_2^-(NH_3)_2$ spectrum exhibits an unresolved shoulder on the low electron kinetic energy side of peak A′. In the sections below, we first interpret peaks A and A′ and then peaks B and C.

The photoelectron spectra of the $H^-(NH_3)_n$ cluster ion system, which is closely related to the $NH_2^-(NH_3)_n$ system, are presented in Figure 3 for comparison. The spectra of $H^-(NH_3)_1$ and $H^-(NH_3)_2$ are both dominated by large peaks, again designated

TABLE 1: Peak Positions, Widths, and Intensities for the Photoelectron Spectra of NH_2^-, ND_2^-, $NH_2^-(NH_3)_1$, $ND_2^-(ND_3)_1$, and $NH_2^-(NH_3)_2$[a]

peak labels	peak center positions(eV): c.m. electron kinetic energy	peak center positions(eV): electron binding energy	peak widths: fwhm (eV)	rel int[b]
		NH_2^-		
	1.760	0.780	0.050	
		ND_2^-		
	1.767	0.773	0.043	
		$NH_2^-(NH_3)_1$		
A	1.229	1.311	0.246	1.00
B	0.786	1.754		0.09
C	0.411	2.129		0.02
		$ND_2^-(ND_3)_1$		
	1.236	1.304	0.239	
		$NH_2^-(NH_3)_2$		
A′	0.765	1.775	0.315	

[a] Photon energy = 2.540 eV. [b] Highest intensity peak normalized to 1.00.

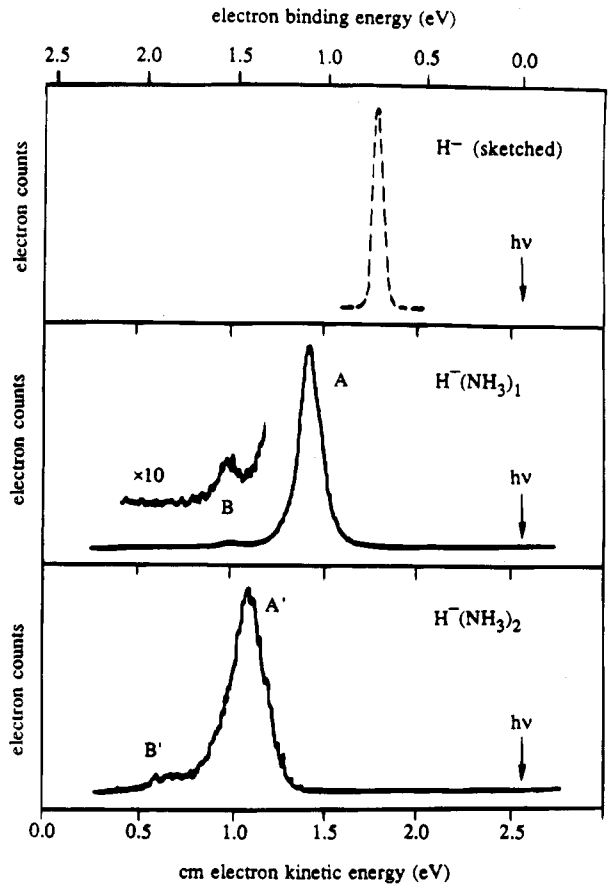

Figure 3. Photoelectron spectra of $H^-(NH_3)_1$ and $H^-(NH_3)_2$, both recorded with 2.540 eV photons. The spectrum of H^- is a single peak, and it has been sketched here for comparison.

as peaks A and A′, respectively, with smaller peaks at lower electron kinetic energies designated as peaks B and B′, respectively. The $H^-(NH_3)_n$ spectra have been described and interpreted in detail previously.[23] Upon analyzing both sets of spectra, we find that qualitatively similar interpretations can explain the general features in both. However, a quantitative comparison reveals significant chemical and structural differences.

2. Peaks A and A′. In preparing to interpret peaks A and A′ in the spectra of $NH_2^-(NH_3)_1$ and $NH_2^-(NH_3)_2$, we should first consider the spectrum of NH_2^- itself. The NH_2^- photoelectron spectrum, which has been studied previously,[26,27] is dominated by a single peak (see Figure 2). Extremely low intensity peaks (<0.7% of this peak's intensity) were also observed on the lower electron kinetic energy side of this peak. Spectroscopic studies have shown that the geometries of the NH_2^- anion and the NH_2 neutral radical are quite similar.[28] The electronic ground states of these two species differ only by the presence of a nonbonding electron in the b_1 orbital of NH_2^-. The photoelectron spectrum of NH_2^- shown in Figure 2 is consistent with these geometric and electronic similarities. The main feature is assigned as the NH_2 ($X\ ^2B_1$, $v' = 0$) ← NH_2^- ($X\ ^1A_1$, $v'' = 0$) vibrational origin transition. The peak is broader than the 30 meV instrumental resolution because it contains unresolved Q, P, and R rotational branches. The maximum of peak A occurs at an electron binding energy of 0.780 ± 0.004 eV, where the error cited is the statistical uncertainty in locating the peak center. This value agrees well with that of a previous study[26] in which the electron binding energy measured from the peak center was reported as $0.779^{+0.013}_{-0.017}$ eV. The energy of the vibrationless, rotationless origin transition, which is equal to the adiabatic electron affinity (EA) of NH_2, may not coincide exactly with the electron binding energy as determined from the peak center. We estimate this difference to be less than ±0.010 eV. In a recent photoelectron investigation of NH_2^- in which the Q, P, and R rotational band contours were resolved,[27] the electron affinity of NH_2 was determined to be $EA(NH_2) = 0.771 \pm 0.005$ eV, in good agreement with the conclusions reached from the NH_2^- photoelectron spectrum shown in Figure 2. The extremely low intensity peaks observed on the low electron kinetic energy side of the main feature in the photoelectron spectrum of NH_2^- are due mainly to transitions to NH_2 with low levels of vibrational excitation in the symmetric stretching and bending modes. Also, a broad, weak peak was observed at electron kinetic energies <0.5 eV. This feature is probably due to transitions to the A $^2A_1$ state of NH_2.

The photoelectron spectra of $NH_2^-(NH_3)_1$ and $NH_2^-(NH_3)_2$ are both dominated by single peaks, i.e., peaks A and A′ in Figure 2. These peaks arise due to photodetachment of electrons from solvated NH_2^- ion "chromophores" within $NH_2^-(NH_3)_1$ and $NH_2^-(NH_3)_2$, respectively. For this reason both peaks resemble the photoelectron spectrum of free NH_2^- except for being broadened and shifted to progressively lower electron kinetic energies owing to the stabilizing effect of solvation. The photoelectron spectra of $NH_2^-(NH_3)_1$ and $NH_2^-(NH_3)_2$ indicate that the excess negative charge is largely localized on a specific component within these cluster ions to form a sub-ion which interacts with the remaining components. Thus, the photoelectron spectra of the resulting ion–molecule complexes may be viewed as the spectra of their perturbed sub-ions. An analogous interpretation has been applied[23] to the photoelectron spectra of the $H^-(NH_3)_{1,2}$ cluster ion series shown in Figure 3.

The electron binding energies of peaks A and A′ are equal to the energy differences between the occupied states of the cluster anion and the states in the Franck–Condon region of the potential energy surface of the corresponding neutral. Little is known about the geometries and potential surfaces of $NH_2^-(NH_3)_1$ and $NH_2^-(NH_3)_2$ and their corresponding neutrals. The van der Waals interactions between constituents of the neutral clusters most likely result in broad, shallow potential surfaces.[29] Consequently, the region of the neutral potential surface accessed by photodetachment, irrespective of the exact geometric configuration, will lie at an energy that does not differ appreciably from the energy of the dissociation asymptote. As a result, the electron-binding energies of peaks A and A′ are

TABLE 2: Summary of Ion–Solvent Dissociation Energies Derived from the Photoelectron Spectra of $NH_2^-(NH_3)_1$, $NH_2^-(NH_3)_2$, $H^-(NH_3)_1$, and $H^-(NH_3)_2$[a]

process	dissociation energy
$NH_2^-(NH_3)_1 \rightarrow NH_2^- + NH_3$	0.54
$NH_2^-(NH_3)_2 \rightarrow NH_2^-(NH_3)_1 + NH_3$	0.46
$H^-(NH_3)_1 \rightarrow H^- + NH_3$	0.36[b]
$H^-(NH_3)_2 \rightarrow H^-(NH_3)_1 + NH_3$	0.35[b]

[a] All values given in electronvolts. [b] See ref 23.

reasonably good approximations to the dissociative detachment energies of $NH_2^-(NH_3)_1$ and $NH_2^-(NH_3)_2$ and to the adiabatic electron affinities of their corresponding neutral complexes.

The electron-binding energy of peak A in the $NH_2^-(NH_3)_1$ photoelectron spectrum is 1.311 eV. As discussed above, this is an approximate measure of the dissociative detachment energy for $NH_2^-(NH_3)_1$, i.e., the energy required for the process

$$NH_2^-(NH_3)_1 \rightarrow NH_2 + NH_3 + e^-$$

Subtracting the electron affinity of NH_2 from the dissociative detachment energy of $NH_2^-(NH_3)_1$ yields the ion–solvent dissociation energy for $NH_2^-(NH_3)_1$ dissociating into NH_2^- and NH_3. This value, $D_0[NH_2^-(NH_3)_1]$, is 0.54 eV. The ion–solvent dissociation energy of $NH_2^-(NH_3)_1$ is a physical quantity of fundamental interest because it is a measure of the strength of the interaction between NH_2^- and a single NH_3 solvent molecule. Theoretical calculations by Squires[30] have suggested a value of 0.52 eV for the ion–solvent dissociation energy of $NH_2^-(NH_3)_1$, in agreement with these results. Castleman[21] has pointed out that $NH_2^-(NH_3)_1$ is isoelectronic to $F^-(NH_3)_1$ and that it too has an ion–solvent dissociation energy of ~0.5 eV. By analogous reasoning, the ion–solvent dissociation energy for $NH_2^-(NH_3)_2$ dissociating into $NH_2^-(NH_3)_1$ and NH_3 is given by the difference in the electron-binding energies of peaks A′ and A. This value, $D_0[NH_2^-(NH_3)_2]$, is 0.46 eV, indicating a slightly smaller stabilization by the second NH_3 solvent molecule.

The ion–solvent dissociation energies for $H^-(NH_3)_1$ and $H^-(NH_3)_2$ were extracted from the photoelectron spectra shown in Figure 3 as described in ref 23. In order to facilitate comparison between the $NH_2^-(NH_3)_n$ and $H^-(NH_3)_n$ cluster ion systems, the ion–solvent dissociation energies for both systems are collected together in Table 2.

The full widths at half maximum of peaks A and A′ are 0.246 and 0.315 eV, respectively, considerably broader than the 0.030 eV instrumental resolution. The width of the peak analogous to peak A in the $ND_2^-(ND_3)_1$ photoelectron spectrum is 0.239 eV, not greatly different from that in the $NH_2^-(NH_3)_1$ spectrum. The broadening of these peaks in the cluster ion spectra is probably due to contributions from several sources including (a) excited weak-bond vibrations in the cluster ions, (b) vibrational excitations in the resulting neutrals, and/or (c) access to a repulsive portion of the neutral's potential surface. These broadening mechanisms are discussed in greater detail in ref 23.

3. Peaks B and C. Peaks B and C in the photoelectron spectrum of $NH_2^-(NH_3)_1$ are primarily due to the excitation of stretching modes in the ammonia solvent during photodetachment. Within the $NH_2^-(NH_3)_1$ ion–molecule complex, the NH_2^- ion interacts with its NH_3 solvent and distorts it from its equilibrium geometry. This creates some Franck–Condon overlap between the distorted ammonia in the ion–molecule complex and the vibrationally excited modes of NH_3 in the resultant neutral. The intensities of peaks B and C relative to peak A is an indication of the degree of distortion of the NH_3 moiety within the cluster ion.

The above assignment of peaks B and C is supported by comparing the spacings between peaks A, B, and C with the stretching frequencies of the free NH_3 molecule,[31] by examining the isotope shifts in the $ND_2^-(NH_3)_1$ spectrum, and by comparison to the photoelectron spectra of the $H^-(NH_3)_n$ cluster ion series.[23] The spacing between peaks A and B in the $NH_2^-(NH_3)_1$ photoelectron spectrum is 3570 ± 120 cm^{-1}, where the cited error is a conservative estimate of the uncertainty in determining the difference between peak centers. The spacing between peaks B and C is 3000 ± 150 cm^{-1}. In NH_3, the band center for the asymmetric stretch occurs at 3443 cm^{-1} while that for the symmetric stretch occurs at 3336 cm^{-1}. Although the locations and intensities of peaks B and C are highly reproducible, these are not sharp peaks. Nevertheless, the A–B peak spacing is reasonably close to an NH_3 stretching frequency. Likewise, the B–C peak spacing is not far from an NH_3 stretching frequency. There may also be minor contributions to peaks B and C from excitation of NH_3 bending modes upon photodetachment; however, it appears that, if present, these contributions are less intense and only serve to broaden the peaks.

In the $ND_2^-(ND_3)_1$ photoelectron spectrum, the main peak occurs at nearly the identical electron binding energy as peak A in the spectrum of $NH_2^-(NH_3)_1$. The peaks analogous to peaks B and C in the $ND_2^-(ND_3)_1$ spectrum, however, have shifted substantially closer to the main peak. This observation confirms peak A as the origin and supports the assignment of peaks B and C as being due to the excitation of NH_3 stretching modes during photodetachment.

In the $H^-(NH_3)_1$ photoelectron spectrum, a peak analogous to peak B in the $NH_2^-(NH_3)_1$ spectrum is also observed. (It, too, is designated as peak B; see Figure 3.) The spacing between this peak and the main peak is also close to the energy of an NH_3 stretching frequency. Furthermore, in the $H^-(NH_3)_1$ spectrum, there is less uncertainty in ascertaining the spacing between peaks since the broadening of the main peak is less pronounced. This makes it possible to assign a specific vibrational mode to this spacing, the NH_3 asymmetric stretch. In the $D^-(ND_3)_1$ photoelectron spectrum, its peak B shifts closer to its main peak (its peak A) by the appropriate amount, in consonance with the proposed interpretation.

The peaks in both the $NH_2^-(NH_3)_1$ and $H^-(NH_3)_1$ photoelectron spectra assigned to excitation of stretching modes in the NH_3 moiety are direct manifestations of the complexation-induced distortion of the NH_3 solvent by its anion. The intensities of these peaks are a measure of the extent to which the NH_3 moiety in the cluster ion is distorted. If the NH_3 moiety in the cluster anion were not distorted, transitions leading to vibrational excitation in NH_3 modes would not have appreciable Franck–Condon factors. In the $NH_2^-(NH_3)_1$ spectrum, the intensity of peak B is ~9% that of peak A, while in the $H^-(NH_3)_1$ spectrum this ratio is only ~3%. This is consistent with the ion–solvent dissociation energy of $H^-(NH_3)_1$ being less than that of $NH_2^-(NH_3)_1$ (see Table 2). Thus, H^- interacts with NH_3 more weakly and distorts it less than does NH_2^-. These findings are also consistent with structural calculations[30] which predict a small solvent distortion in $H^-(NH_3)_1$, yet a significant elongation of an ammonia N–H bond in $NH_2^-(NH_3)_1$.

Discussion

The clustering of solvent molecules around a bare gas phase anion stabilizes the excess negative charge on the ion, and this results in a decrease in its gas phase basicity. The ordering of

relative basicities in the gas phase often differs from their ordering in solution.[17] This observation underscores the important role played by the solvent in determining the energetics involved in solution phase chemistry and the value of studying bare ions in the gas phase to determine their intrinsic chemical properties. Partially solvated ions afford a means of studying the transition between bare ions in the gas phase and solvated ions in condensed phases. Below, the gas phase basicities of NH_2^- and H^- will be computed as a function of the number of NH_3 solvent molecules by using ion−solvent dissociation energies derived from our cluster ion photoelectron spectra.

The gas phase basicity, $GB(A^-)$, of a negative ion, A^-, is defined[6] as the free energy change for the reaction

$$AH \rightarrow A^- + H^+ \qquad \Delta G = GB(A^-)$$

The gas phase acidity, $H_{acid}(HA)$, of the conjugate acid, AH, is defined[5] as the enthalpy change for the same reaction:

$$AH \rightarrow A^- + H^+ \qquad \Delta H = H_{acid}(HA)$$

Since ΔG and ΔH for a reaction differ only by the term $-T\Delta S$, at low temperatures the gas phase acidity of AH will be approximately equal to the gas phase basicity of its conjugate base, A^-. At 0 K, these quantities are formally equal.

The H^- ion and the NH_2^- ion are both strong bases and have similar gas phase basicities. By using flow tube techniques to study the reaction $NH_2^- + H_2 \rightarrow H^- + NH_3$, Bohme[13] definitively showed, however, that in the gas phase NH_2^- is a stronger base than H^-. The gas phase acidity of NH_3 at 0 K has been calculated by Wickham-Jones et al.[27] by using their experimentally measured value of $EA(NH_2) = 0.771 \pm 0.005$ eV in eq 1:

$$H_{acid,0K}(NH_3) = D_0(H-NH_2) + IP(H) - EA(NH_2) \quad (1)$$

where $D_0(H-NH_2) = 106.7 \pm 0.3$ kcal/mol is the ammonia bond dissociation energy[32] and $IP(H) = 313.59 \pm 0.01$ kcal/mol is the ionization potential of the hydrogen atom.[33] The value calculated in this way is $H_{acid,0K}(NH_3) = 402.5 \pm 0.4$ kcal/mol, and it agrees with the gas phase equilibrium value of $H_{acid,298K}(NH_3) = 403.6 \pm 0.8$ kcal/mol. The gas phase acidity of H_2 at 0 K may be calculated in a similar manner:

$$H_{acid,0K}(H_2) = D_0(H_2) + IP(H) - EA(H) \quad (2)$$

where $D_0(H_2) = 103.27$ kcal/mol[34] and $EA(H) = 17.39$ kcal/mol is the electron affinity of the hydrogen atom.[35] The value derived in this way is $H_{acid,0K}(H_2) = 399.47 \pm 0.01$ kcal/mol, in reasonable agreement with the gas phase equilibrium value of $H_{acid,298K}(H_2) = 400.4 \pm 0.5$ kcal/mol.[36] As mentioned earlier, at 0 K, the gas phase acidity of AH is equal to the gas phase basicity of the conjugate base A^-. Thus, the gas phase basicities at 0 K of NH_2^- and H^- are 402.5 ± 0.4 and 399.47 ± 0.01 kcal/mol, respectively. Note that higher gas phase basicity values are associated with stronger bases. The gas phase basicity values of NH_2^- and H^- given above support Bohme's conclusion[13] that the bare NH_2^- ion is more basic than the bare H^- ion in the gas phase.

The gas phase basicity of $NH_2^-(NH_3)_1$ is obtained from

$$GB_{0K}[NH_2^-(NH_3)_1] = D_0[(NH_3)_2] + D_0(H-NH_2) + IP(H) - EA(NH_2) - D_0[NH_2^-(NH_3)_1] \quad (3)$$

where $D_0[(NH_3)_2]$ is the van der Waals dissociation energy of the neutral ammonia dimer and the other quantities have been defined previously. The van der Waals dissociation energy of the ammonia dimer is probably about an order of magnitude smaller than any of the other quantities in eq 3, and it is assumed here to be negligible.[29] Using $D_0[NH_2^-(NH_3)_1] = 0.54$ eV gives a value of $GB_{0K}[NH_2^-(NH_3)_1] = 390$ kcal/mol. The gas phase basicities of $H^-(NH_3)_1$, $NH_2^-(NH_3)_2$, and $H^-(NH_3)_2$ were calculated in an analogous fashion. All of the gas phase basicity values calculated in this way are summarized in Table 3 and plotted as a function of the number of NH_3 solvent molecules in Figure 4.

TABLE 3: Summary of Gas Phase Basicity Values[a]

ion	GB_{0K}	ref	ion	GB_{0K}	ref.
NH_2^-	402.5 ± 0.4	28	H^-	399.47 ± 0.01	see text
$NH_2^-(NH_3)_1$	390 ± 2	this work	$H^-(NH_3)_1$	392 ± 2	23
$NH_2^-(NH_3)_2$	379 ± 2	this work	$H^-(NH_3)_2$	384 ± 2	23

[a] All values given in kcal/mol.

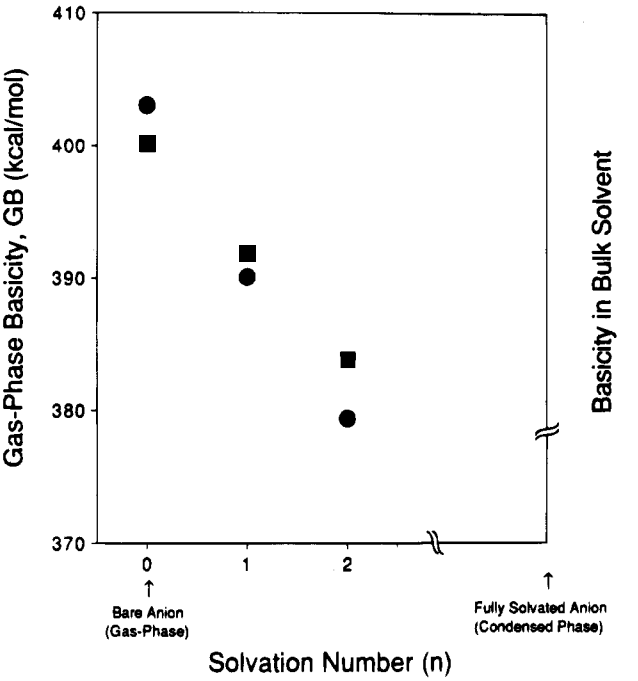

Figure 4. Gas phase basicity values for $H^-(NH_3)_{n=0-2}$ [■] and $NH_2^-(NH_3)_{n=0-2}$ [●], plotted as a function of solvation number.

These results show that the gas phase basicities of H^- and NH_2^- decrease as they are solvated by ammonia. While the bare NH_2^- ion is a stronger base than the bare H^- ion, the addition of only two NH_3 solvent molecules is sufficient to reverse the relative basicities of these species. Upon association with one ammonia molecule, the gas phase basicities of the amide and the hydride ions become comparable. Upon association with two ammonia molecules, however, the gas phase basicity of the hydride ion exceeds that of the amide ion by 4.5 kcal/mol. The primary factor responsible for this reversal is that the NH_2^- ion interacts more strongly with NH_3 than does the H^- ion, resulting in greater changes in the basicity of NH_2^- upon addition of each solvent molecule. This makes the slope of the plot of the amide data in Figure 4 steeper than that of the hydride data, and this is at the heart of the reason for the switchover in basicity ordering. While the basicities of $H^-(NH_3)_{1,2}$ and $NH_2^-(NH_3)_{1,2}$ determined in this work are still far from converging to the basicity values of hydride and amide ions in bulk ammonia solvent, it is clear that only a few ammonia solvent molecules are necessary to switch around the ordering of basicities in these systems. Related studies by Bohme and colleagues[11,37,38] have also demonstrated the im-

portant role played by specific interactions between anion and solvent molecules. In their flow-tube studies, the relative basicities of OH^- and CH_3O^-, for instance, were found to reverse upon addition of two CH_3OH solvent molecules, while with H_2O as the solvent, even three molecules were not sufficient to induce the switch. The results reported in the present paper, along with those of Bohme, have significance for chemists because they emphasize that ion−solvent complexes containing only a few solvent molecules can serve as useful models for describing some of the main qualitative features of ion solvation.

Acknowledgment. We wisk to thank D. K. Bohme, A. W. Castleman, Jr., M. Henchman, M. Jones, S. A. Lyapustina, C. R. Moylan, and R. R. Squires for helpful discussions. We gratefully acknowledge the support of the National Science Foundation under Grants CHE 8511320 and CHE 9007445.

References and Notes

(1) Reichardt, C. *Solvent and Solvent Effects in Organic Chemistry,* 2nd ed.; VCH: New York, 1988.
(2) Waddington, T. C. *Non-Aqueous Solvents*; Appleton-Century-Crafts: New York, 1969.
(3) Smith, H. *Chemistry in Non Aqueous Ionizing Solvents, Vol. I Chemistry in Anhydrous Liquid Ammonia, Parts 1 and 2*; Interscience: New York, 1963.
(4) McIver, R. T. *Sci. Am.* **1980**, *243*, 148.
(5) Bartmess, J. E.; McIver, R. T. In *Gas Phase Ion Chemistry*, Bowers, M. T., Ed.; Academic: New York, 1979; *Vol. 2*, p 87.
(6) Aue, D. H.; Bowers, M. T. In *Gas Phase Ion Chemistry*; Bowers, M. T., Ed.; Academic: New York, 1979; *Vol. 2*, p 1.
(7) Lehman, T. A.; Bursey, M. M. *Ion Cyclotron Resonance Spectrometry*; Wiley-Interscience: New York, 1976.
(8) Munson, M. S. B. *J. Am. Chem. Soc.* **1965**, *87*, 2332. Kebarle, P. *Ions and Ion Pairs in Organic Reactions*; Wiley-Interscience: New York, 1972; *Vol. 1*, p 27.
(9) Bohme, D. K. In *Interactions between Ions and Molecules*; Auslos, P., Ed.; Plenum: New York, 1974; p 489.
(10) Moylan, C. R.; Brauman, J. I. *Annu. Rev. Phys. Chem.* **1983**, *34*, 187.
(11) Mackay, G. I.; Bohme, D. K. *J. Am. Chem. Soc.* **1978**, *100*, 327.
(12) Lau, Y. K.; Kebarle, P. *Can. J. Chem.* **1981**, *59*, 151.
(13) Bohme, D. K.; Hemsworth, R. S.; Rundle, R. W. *J. Chem. Phys.* **1973**, *59*, 77.
(14) Brauman, J. I.; Blair, L. K. *J. Am. Chem. Soc.* **1968**, *90*, 6561; **1970**, *92*, 5986.
(15) Munson, M. J. B. *J. Am. Chem. Soc.* **1965**, *87*, 2332.
(16) Bartmess, J. E. *Mass Spectrom. Rev.* **1989**, *8*, 297.
(17) Keesee, R.; Lee, N.; Castleman, A. W., Jr. *J. Chem. Phys.* **1980**, *73*, 2195.
(18) Kebarle, P.; Davidson, W. R.; Sunner, J.; Meza-Höjer, S. *Pure Appl. Chem.* **1979**, *51*, 63.
(19) Bohme, D. K. In *Ionic Processes in the Gas Phase*; Almoster Ferreira, M. A., Ed.; D. Reidel: New York, 1984.
(20) Kebarle, P. *Annu. Rev. Phys. Chem.* **1977**, *28*, 445.
(21) Castleman, A. W., Jr.; Märk, T. D. In *Gaseous Ion Chemistry and Mass Spectrometry*; Futrell, J., Ed.; Wiley: New York, 1986; p 259.
(22) Keesee, R. G.; Castleman, A. W., Jr. *J. Phys. Chem. Ref. Data* **1986**, *15*, 101.
(23) Snodgrass, J. T.; Coe, J. V.; Freidhoff, C. B.; McHugh, K. M.; Bowen, K. H. *Faraday Discuss. Chem. Soc.* **1988**, *86*, 241.
(24) Coe, J. V.; Snodgrass, J. T.; Freidhoff, C. B.; McHugh, K. M.; Bowen, K. H. *J. Chem. Phys.* **1987**, *87*, 4302.
(25) Coe, J. V.; Snodgrass, J. T.; Freidhoff, C. B.; McHugh, K. M.; Bowen, K. H. *J. Chem. Phys.* **1986**, *84*, 618.
(26) Cellota, R. J.; Bennett, R. A.; Hall, J. L. *J. Chem. Phys.* **1974**, *60*, 1740.
(27) Wickham-Jones, C. T.; Ervin, K. M.; Ellison, G. B.; Lineberger, W. C. *J. Chem. Phys.* **1989**, *91*, 2762.
(28) Tack, L.; Rosenbaum, N.; Owrutsky, J.; Saykally, R. *J. Chem. Phys.* **1986**, *84*, 7056.
(29) Nelson, D. D.; Klemperer, W.; Fraser, G. T. *J. Chem. Phys.* **1987**, *87*, 6364.
(30) Squires, R. R. In *Ionic Processes in the Gas Phase*; Almoster Ferreira, M. A., Ed.; D. Reidel: New York, 1984.
(31) Hertzberg, G. *Molecular Spectra and Molecular Structure*; Van Nostrand: New York, 1966; Vol. 3. Spirko, V. *J. Mol. Spectrosc.* **1983**, *101*, 30. Urban, S.; Spirko, V.; Papousek, D.; McDowell, R. S.; Nereson, N. G.; Belov, S. P.; Gershstein, L. I.; Maslovsky, A. V.; Krupnov, A. S.; Curtis, J.; Rao, K. N. *J. Mol. Spectrosc.* **1980**, *79*. 455. Angstl, R.; Finsterhoylz, H.; Frunder, H.; Illig, D.; Papousek, D.; Pracna, P.; Rao, K. N.; Schrotter, H. W.; Urban, S. *J. Mol. Spectrosc.* **1985**, *114*, 454. Benedict, W. S.; Plyler, E. K. *Can. J. Phys.* **1957**, *35*, 1235.
(32) Gibson, S. T.; Greene, J. P.; Berkowitz, J. *J. Chem. Phys.* **1985**, *83*, 4319.
(33) Chase, M. W., Jr.; Davies, C. A.; Downey, J. R., Jr.; Frurip, D. J.; McDonald, R. A.; Sguerud, A. N. *J. Phys. Chem. Ref. Data* **1986**, *15*, (Suppl. 1), 101.
(34) Herzberg, G. *J. Mol. Spectrosc.* **1970**, *33*, 147.
(35) Mead, R. D.; Stevens, A. E.; Lineberger, W. C. In *Gas Phase Ion Chemistry*; Bowers, M. T., Ed.; Academic: New York, 1984; Vol. 3.
(36) Bartmess, J. E.; McIver, R. T. In *Gas Phase Ion Chemistry*; Bowers, M. T., Ed.; Academic: New York, 1979; *Vol. 2*, p 90.
(37) Bohme, D. K.; Rakshit, A. B.; Mackay, G. I. *J. Am. Chem. Soc.* **1982**, *104*, 1100.
(38) Mackay, G. I.; Rakshit, A. B.; Bohme, D. K. *Can. J. Chem.* **1982**, *60*, 2594.

JP943052H